Effect of Hemimethylation and Methylation of Adenine on the Structure and Stability of Model DNA Duplexes†

Qiu Guo,‡ Min Lu,§ and Neville R. Kallenbach*

Department of Chemistry, New York University, New York, New York 10003

Received June 14, 1995; Revised Manuscript Received October 20, 1995⊗

ABSTRACT: Enzymatic methylation of adenine underlies a variety of biological regulatory mechanisms in *Escherichia coli.* We present here structural and thermodynamic characterization of a non-self-complementary DNA decamer duplex containing the *dam* sequence 5′-GATC in the unmethylated, hemimethylated (both forms), and methylated states. Differential scanning calorimetry measurements show that the free energies for adenine methylation of the decamer duplex are +1.1 and +2.0 kcal/mol for hemimethylation, respectively, and +3.3 kcal/mol for full methylation. In all cases, a large unfavorable enthalpy change is partially compensated by a favorable entropy term. CD spectroscopy indicates an overall conformational difference between the unmethylated decamer duplex and its methylated analogs. Reaction with diethyl pyrocarbonate (DEPC), a purine-specific probe sensitive to conformation, is enhanced in the vicinity of the methylation site of the duplex, consistent with loosening of base pairing at this site. Comparison of the scission patterns of these decamer duplexes by the reactive probes methidiumpropyl-EDTA·Fe^{II} [MPE·Fe^{II}] and Cu^{I}(*o*-phenanthroline)$_2$ [$(OP)_2Cu^{I}$] indicates that the methylation site of the decamer duplex represents a site of enhanced reactivity for these agents. On the basis of these thermodynamics and structural features, we suggest that the methylated base pair exists in two different helical states, which require local transient opening of the duplex for interconversion.

Enzymatic methylation of nucleic acids at the nucleotide bases effectively increases the amount of information that many organisms can encode in their genome. It underlies a variety of biological regulatory mechanisms (Derosiers et al., 1974). The molecular basis of many of these methylation-dependent regulations has not been defined. The *dam* methyltransferase of *E. coli* methylates the N6 position of adenine on both strands of the symmetrical sequence 5′-GATC (Geier & Modrich, 1979). It acts primarily on hemimethylated substrates (Pukkila et al., 1983). Following passage of the replication fork, a GATC site is transiently hemimethylated until newly synthesized strands become methylated by *dam* methytransferase (Marinus, 1976; Lyons & Schendel, 1984). This period of hemimethylation is crucial for several biological processes in *E. coli*, including mismatch DNA repair (reviewed in Modrich, 1987), regulation of DNA transposition (Roberts et al., 1985), and control of DNA replication initiation (Russell & Zinder, 1987).

In principle, the presence of a methyl group on the N6 position of adenine offers a well defined and distinctive target for selective protein-nucleic acid recognizing interactions (Rosenberg et al., 1973). This notion is supported by the observation that IS10 transposition activity is increased when two GATC sites in IS10 are unmethylated as well as when they are hemimethylated; one hemimethylated form of IS10 is estimated to be 300 times more active than the other (Roberts et al., 1985). These observations also imply that the structural perturbations by adenine methylation are different between the template and nontemplate strands. Recently, *E. coli* SeqA protein, a negative regulator of replication origin function, has been demonstrated to bind specifically to the fully methylated DNA replication origin (Lu et al., 1994; Slater et al., 1995).

How does adenine hemimethylation or methylation affect the local conformation of the duplex DNA containing a *dam* site? While recognition does not demand changes in local structure, restriction or modification enzymes might nevertheless sense conformational signals present in the target sequence as well as the methyl group itself. For example, the N6 methyl group on monomeric adenine strongly favors the rotamer *cis* to N1, which is incompatible with Watson−Crick pairing (Engel & von Hippel, 1974). Biophysical studies on duplexes formed by copolymers of m^6A and A, and poly dT indicate destabilization of the methylated structures relative to the unmethylated species, with no obvious conformational effect at low temperatures (Engel & von Hippel, 1978). NMR experiments have attempted to define the role of the methyl group on the local structure of duplexes in more detail. No structural differences between the unmethylated, hemimethylated, or methylated species could be discerned. However, the results confirm a consistent destabilization of methylated duplexes relative to the unmethylated sequences (Fazakerley et al., 1984, 1985, 1987; Quignard et al., 1985a,b; Rinkel et al, 1987a,b). Specifically, the ^1H NMR results suggest the presence of at least one intermediate structure between the duplex and coils in the case of a hemimethylated sequence, G^{m}ATC, but not its complement (Fazakerley et al., 1987). While it is argued that the intermediate is not a hairpin, the structure of the intermediate remains to be determined (Fazakerley et al., 1987). No *syn* nucleotides have been detected in the oligonucleotide complexes studied at low temperatures,

† This work was supported by Grant CA 24101 from the U.S. National Institutes of Health.

* Author to whom correspondence should be addressed.

‡ Present address: Massachusetts Institute of Technology, Department of Biology, Cambridge, MA 02139.

§ Present address: Whitehead Institute for Biomedical Research, Cambridge, MA 02142.

⊗ Abstract published in *Advance ACS Abstracts,* December 1, 1995.

0006-2960/95/0434-16359$09.00/0

Scheme 1. GATC Strands with A* Denoting N^6-Methyl-2′-deoxyadenosine

A: 5′-C--G--C--G--A--T--C--C--G--C-3′

A^c: 5′-G--C--G--G--A--T--C--G--C--G-3′

mA: 5′-C--G--C--G--A*-T--C--C--G--C-3′

mA^c: 5′-G--C--G--G--A*-T--C--G--C--G-3′

suggesting that Hoogsteen base pairs do not arise (Fazakerley et al., 1984). Since, as Engel and von Hippel (1974) point out, the intrinsic stability of Hoogsteen pairs is close to that of Watson–Crick pairs, the destabilization of DNA by methylation of adenine without forming Hoogsteen pairs poses an interesting problem. Possibly, differential hydration of the two base pairs might play a role. Important aspects of the role of adenine methylation in the structure and dynamics of duplex DNA containing the *dam* sequence remain to be clarified.

We report here thermodynamic and structural studies of four non-self-complementary decamers containing the *dam* sequence in unmethylated, hemimethylated, and methylated states (Scheme 1).

The sequence is chosen to minimize hairpin formation by restricting self-complementation in the flanking G·C pairs. We show here that the destabilization by m^6A does not involve differential ionic interactions, as seen from the dependence of the T_m on salt. On the basis of CD spectroscopy and footprinting experiments, we detect structural differences between the unmethylated control and the two hemimethylated duplexes, and between these and the fully methylated duplex. Each duplex has a distinct CD spectrum, and each responds differently to chemical probes of the strands. These results suggest that the conformation of each duplex is therefore different in the vicinity of the methylation site.

MATERIALS AND METHODS

Synthesis and Purification of Oligonucleotides. N^6-Methyl-2′-deoxyadenosine was purchased from Glen Research. Oligonucleotides used in this study were synthesized on an ABI 391 PCR-Mate EP DNA synthesizer and deprotected by routine phosphoramidite procedures (Caruthers, 1982). Strands were purified by preparative HPLC on a Du Pont Zorbax Bio Series oligonucleotide column, following the manufacturer's recommended elution protocol. Oligonucleotides were labeled at their 5′-termini using T4 polynucleotide kinase (Boehringer), and the labeled strands were purified by polyacrylamide gel electrophoresis. Extinction coefficients of the DNAs in single strands were measured with melting curves by extrapolation to 80 °C of the molar extinctions calculated using the nearest-neighbor values of Cantor et al. (1970). The concentration of DNA strands was determined with use of the following extinction coefficients in single strands at 80 °C: $A_{260} = 9.804 \times 10^4$ for A and mA; $A_{260} = 9.075 \times 10^4$ for A^c and mA^c.

Annealing Reactions. A stock solution of decamer duplex was prepared by annealing a stoichiometric mix of strands in 20 μL of 10 mM sodium phosphate, pH 7, 0.1 mM EDTA, and 100 mM NaCl. An Eppendorf tube containing the solution was immersed in boiling water for 2 min, cooled slowly to room temperature, and finally chilled to 4 °C.

Ultraviolet Melting Curves. All DNA solutions were prepared in 10 mM sodium phosphate, pH 7, 0.1 mM EDTA, 100 mM NaCl. Absorbance *versus* temperature profiles were measured at 260 nm on a Perkin-Elmer 575 spectrophotometer interfaced to a PC-XT computer for acquisition and analysis of experimental data. The temperature of the cell holder was thermoelectrically controlled and programmed. Samples were heated at a rate of 0.5 °C/min. Absorbance and the temperature were recorded every 0.5 min. These melting curves allow us to measure the transition temperature (T_m), which are the midpoints of the order–disorder transition of these DNA molecules, as well as the relevant thermodynamic parameters. These parameters were calculated using standard procedures (Marky & Breslauer, 1987) which correspond to an all-or-none approximation of the helix–coil transition of each molecule.

Differential Scanning Calorimetry (DSC). The excess heat capacity as a function of temperature for each duplex was measured with a Microcal MC-2 differential scanning calorimeter. The DNA solution was scanned against the same buffer from 15 to 100 °C at a heating rate of 45 °C/h. For the analysis of the experimental data, a buffer *vs* buffer scan is subtracted from the sample *vs* buffer scan; both scans in the form of millicalories per second *vs* temperature were converted to millicalories per degree Celsius *vs* temperature by dividing each experimental data point by the corresponding heating rate. The area under the resulting curve is proportional to the total heat of the transition and when normalized for the number of millimoles is equal to the transition enthalpy, Δh_{cal}. Analysis of the shape of the thermal absorption profile results in a second set of van't Hoff heat and entropy values, which are indicated in Table 1 as "DSC" derived values to distinguish them from the van't Hoff values derived from optical transition data.

CD Spectroscopy and CD Melting Curves. Circular dichroism spectra were recorded using an AVIV model 60DS CD spectropolarimeter equipped with a programmable, thermoelectrically controlled cell holder (AVIV Associates, Lakewood, NJ). DNA solutions were prepared in 10 mM sodium phosphate, pH 7, 0.1 mM EDTA, 100 mM NaCl. Each spectrum corresponds to an average of three scans from which the buffer background was subtracted.

Footprinting Experiments. DNAs were reacted with diethyl pyrocarbonate (DEPC) as described by Herr (1985) and Lu et al. (1990). MPE·Fe^{II} cleavage was based on those of van Dyke and Dervan (1983) and Guo et al. (1989). The DNAs were reacted with $(OP)_2Cu^I$ at 4 °C for 45 min as described previously (Guo et al., 1990).

Gel Electrophoresis. Native (20%) polyacrylamide gels were run at 4 °C for 20 h at 100 V (approximately 8 V/cm). The electrophoresis plates were jacketed and cooled with circulating water to provide a running temperature of 4 °C in the gel during the electrophoresis. The buffer system contained 40 mM Tris, 20 mM acetic acid, 1 mM EDTA, at pH 8.1. No tracking dyes were added to samples in the runs. For denaturing gels, samples of products of cleavage reactions were taken up in formamide loading buffer, heated briefly to 90 °C, cooled, then run on a 24% denaturing polyacrylamide gel for 4 h at 2000 V (ca 50 V/cm) and 40 °C. The gel was dried immediately on a vacuum drying apparatus (Hoefer), and exposed at room temperature to X-ray film without an intensifier screen. Autoradiograms were analyzed quantitatively by densitometry of bands using a computing densitometer from Molecular Dynamics. No base line corrections are applied. The data from the experiments we report consist of profiles corresponding to the relative probability of chain scission at a series of

Table 1: Thermodynamic Parameters for Complex Formation in GATC Oligonucleotides

		$\Delta G°_{25}$, kcal mol^{-1}			D$H°$, kcal mol^{-1}			$T\Delta S°_{25}$, kcal mol^{-1}		
	T_m (°C), 10^{-5} M	cal[a]	vH[b]	T_m^{-1} vs ln C_T[c]	cal	vH	T_m^{-1} *vs* ln C_T	cal	vH	T_m^{-1} vs ln C_T
A/A^c	59.2	-19.0 ± 1.1[d]	-14.7 ± 0.9	-14.8 ± 0.8	-102.1 ± 2.8	-69.1 ± 1.8	-70.0 ± 2.5	-83.1 ± 3.9	-54.4 ± 2.7	-55.2 ± 3.3
		(-13.0 ± 0.7)[e]				(-50.7)DSC				
mA/A^c[f]	55.5	-16.9 ± 0.9	-14.1 ± 0.8	-14.2 ± 0.7	-90.0 ± 1.5	-69.1 ± 6.5	-70.8 ± 4.6	-73.1 ± 2.4	-55.0 ± 7.3	-56.6 ± 5.3
		(-11.0 ± 0.6)				(-50.8)DSC				
A/mA^c[g]	54.1	-17.0 ± 1.0	-13.3 ± 0.8	-13.3 ± 0.7	-92.7 ± 0.4	-63.3 ± 5.0	-63.6 ± 3.7	-75.7 ± 1.4	-50.0 ± 5.8	-50.3 ± 4.4
		(-11.1 ± 0.6)				(-50.6)DSC				
mA/mA^c	50.6	-15.7 ± 0.8	-12.2 ± 0.7	-12.9 ± 0.7	-86.8 ± 1.0	-59.4 ± 2.6	-66.0 ± 5.2	-71.1 ± 1.8	-47.2 ± 3.3	-53.2 ± 5.9
		(-9.8 ± 0.5)				(-50.6)DSC				

[a] Calorimetric values. [b] Curve fit values. [c] Concentration dependence of T_m values. [d] $\Delta S° = R \ln(4/C_T) + \Delta H°/T_m$, $\Delta G = \Delta H - T\Delta S$. [e] $\Delta G = \Delta H(1 - T/T_m)$. [f] Hemimethylation of the template strand. [g] Hemimethylation of the non-template strand.

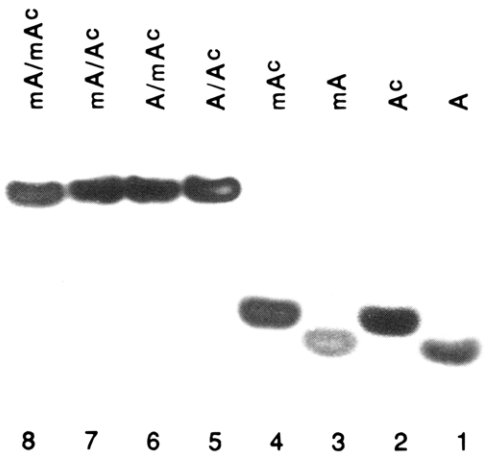

FIGURE 1: Native gel electrophoretic analysis of duplex formation of decamer stands in unmethylated, hemimethylated, and fully methylated states at 4 °C. Each lane contains the indicated single strand (see Scheme 1) or an equimolar mixture of two strands after annealing (see Materials and Methods).

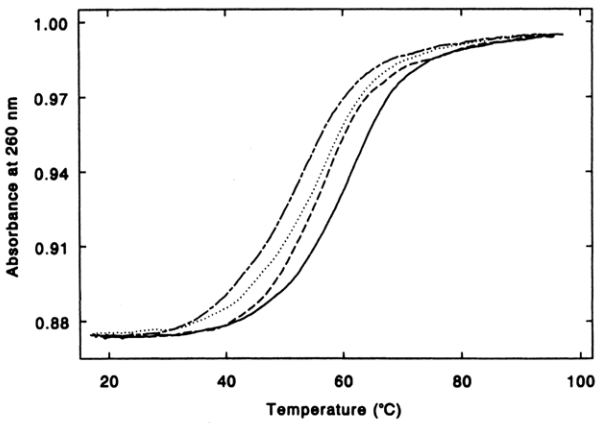

FIGURE 2: Thermal UV melting of the decamer duplexes in unmethylated, hemimethylated, and fully methylated states. Melting was monitored by changes in UV absorbance at 260 nm (see Materials and Methods). UV melting profiles for GATC duplexes A/A^c (solid line), mA/A^c (dashed line), A/mA^c (dotted line), and mA/mA^c (−•−) in 10 mM sodium phosphate, pH 7, 0.1 mM EDTA, 100 mM NaCl. The total DNA strand concentration is 5 μM. Samples were pre-equilibrated at 4 °C for 1 h.

positions with respect to a labeled 5′-phosphate for each strand in a DNA decamer duplex. These profiles can differ in the overall intensity of scission as well as in the relative intensity at individual bands. We use the band at position 9 as a standard to normalize each profile. This band lies near the chain terminus, where effects from the adenine methylation might be expected to be less evident.

RESULTS

Formation of a Defined Decamer Duplex DNA Structure. We attempt here to understand how adenine hemimethylation and complete methylation affects the local structure of a DNA duplex. Accordingly, we synthesized four decamer strands (see Scheme 1) that were designed to form non-self-complementary duplexes in unmethylated, hemimethylated, and fully methylated states. Electrophoretic mobilities of equimolar mixtures of the decamer strands in four possible combinations under native conditions at 4 °C are shown in Figure 1. Each pair of DNA strands migrates as a duplex, indicating the formation of a defined structure. All four decamer duplexes have similar gel mobilities despite obvious differences in mobility among the free strands (Figure 1). No indication of forming intermediate structure(s) such as hairpins could be found in these gels or in others run after the strands were cooled rapidly following heating and annealing at intermediate temperatures (data not shown).

Thermodynamic Profiles for Destabilization of Decamer Duplex Structure by Adenine Methylation. Thermal unfolding experiments confirm that methylation significantly destabilizes duplex structure. This is evident in the profiles shown in Figure 2, where the midpoint of the transition profiles (T_m values) differ by nearly 10 °C for the fully methylated species relative to the unmodified duplex. We have evaluated the thermodynamics of destabilizing duplex structure by adenine methylation further using differential scanning calorimetry (DSC). Calorimetry allows determination of the transition enthalpy for each duplex without recourse to models of the underlying process (Marky & Breslauer, 1987). The DSC values can be used to extract both intrinsic transition enthalpies, ΔH_{cal}, as well as van't Hoff enthalpies from analysis of the shape of the calorimetric transition profiles (Marky et al., 1987). Table 1 summarizes the thermodynamic data on the four decamer duplexes from the DSC measurements. The free energy (ΔG) for adenine methylation is +1.1 kcal/mol for hemimethylation of the template strand, +2.0 kcal/mol for hemimethylation of the nontemplate strand, and +3.3 kcal/mol for full methylation (Table 1). Moreover, the two hemimethylated duplexes differ in stability by approximately 0.9 kcal/mol and are not equivalent (see Table 1). The lower stability of the hemimethylated and methylated duplexes results from a strong reduction in their enthalpies of formation as well as in the opposing $T\Delta S$ contributions (Table 1). The resultant net free energy difference is small, indicating compensation between the enthalpic and entropic terms.

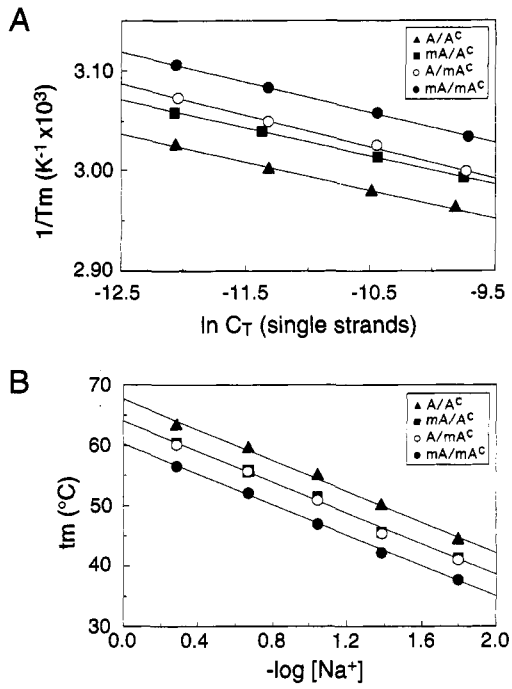

FIGURE 3: (A) Dependence of the transition temperature of the decamer duplexes in unmethylated, hemimethylated, and fully methylated states on strand concentration. (B) Plots of the T_m *versus* $-\log[Na^+]$ in 10 mM sodium phosphate, pH 7, 0.1 mM EDTA.

We estimated the van't Hoff enthalpies of forming the decamer duplexes by fitting the shapes of the thermal and optical transition profiles (Figure 2), and also by measuring the dependence of T_m on strand concentration (Figure 3A). The latter measurement provides a test of the all-or-none nature of the transition, in which T_m^{-1} is predicted to be linear in ln C, where C is the total strand concentration. Thermodynamic parameters derived from the fits of the DSC and optical melting curves as well as the ln C_T plots are summarized in Table 1. The results show that the fully methylated and hemimethylated duplexes are less stable than the unmethylated species (Table 1). In addition, the values for the calorimetrically monitored data are greater than van't Hoff parameters (see Table 1). This feature is not atypical for oligomeric duplexes, and is also retained in the unmethylated duplex, so that it is a characteristic of the sequence and not of methylation. This feature suggests that a transition unit within the decamers acts as a substructure in the decamer. It would be consistent for example with the presence of a partially structured intermediate, in which a unit about the size of a pentamer, representing one-half of the nearly symmetrical sequence of the decamer, unfolds prior to transition of the second.

The destabilization of the decamer duplex DNA by adenine methylation may involve differential ionic interactions. To test this hypothesis, we determined the salt dependence of T_m for the four decamer duplexes. Figure 3B shows plots of T_m versus $\log[Na^+]$. We obtained values of 12.7−12.8 for the slopes of such plots. This weak dependence on salt concentration is characteristic of ion release that occurs in oligomeric duplexes (Erie et al., 1987). These results indicate that the unmethylated decamer duplex and its methylated analogs have similar charge densities, ionic interactions, and counterion release on denaturation.

Adenine Methylation Induces a Conformation Differences. CD spectroscopy provides a sensitive differential probe of overall conformation in DNA oligomers (Tinoco & Cantor, 1970). The CD spectra of duplexes corresponding to unmethylated, hemimethylated and fully methylated sequences were measured at 4 °C, a temperature at which all four molecules form helical structures (Figure 4). The shape of the unmethylated duplex spectrum is characteristic of B-DNA in this wavelength region. The peaks of the spectra of hemimethylated and fully methylated duplexes are slightly shifted compared to that of the unmethylated duplex although the four duplexes have the same trough. The magnitudes of the maxima and minima change with methylation, too (see Figure 4). The spectra of the two hemimethylated duplexes are not identical, implying a difference in local conformation and/or dynamics. Although the difference between these CD spectra is small, they are very reproducible; the error of the determinations is within ±2% from replicate runs. Differences between A/A^c and the methylated species at the peak and trough are therefore significant; the differences among methylated species are within the experimental error.

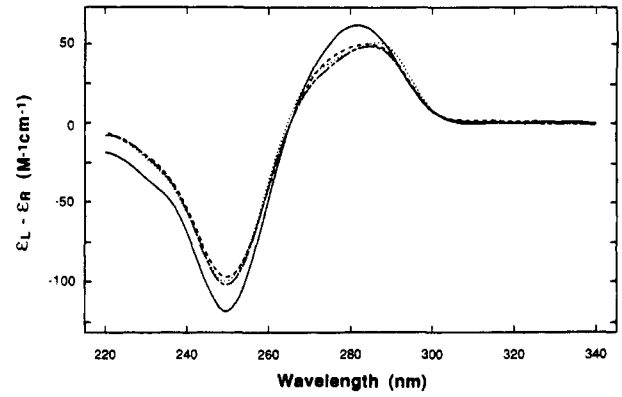

FIGURE 4: CD spectra of the decamer duplexes A/A^c (solid line), mA/A^c (dashed line), A/mA^c (−•−), and mA/mA^c (dotted line) in 10 mM sodium phosphate, pH 7, 0.1 mM EDTA, 100 mM NaCl at 4 °C. The total DNA strand concentration is 50 μM. Samples were preequilibrated at 4 °C for 1 h. Each spectrum corresponds to an average of three scans.

Purine Bases at the Methylation Site Are Reactive to Diethyl Pyrocarbonate. Chemical probes of the structure and conformation of nucleic acids make it possible to investigate details of DNA or RNA structure to a resolution of a single base pair (Gilbert et al., 1976; Singer, 1975). Diethyl pyrocarbonate (DEPC) is a purine specific reagent, with a preference for N7 of A over that of G (Herr, 1985), and is sensitive to local conformation in DNA (Johnston & Rich, 1985). Here we use DEPC to probe the major groove environment at the methylation site of the decamer duplex DNA. We compare the reactivity of the hemimethylated and fully methylated duplexes to DEPC with that of the unmethylated duplex. If m^{6}A compromises mA·T pairing in the decamer duplex, then we should see enhanced reactivity at the methylated A residue. Figure 5 shows the profiles of DEPC reaction of the four decamer duplexes. Both methylated A's in A5 in the fully methylated duplex are very reactive, hence more accessible than in the fully paired control of the unmethylated duplex, A/A^c. This is also seen in the hemimethylated duplex mA/A^c; the other hemimethylated duplex A/mA^c shows slightly more reactivity at A5, relative to the unmethylated control (see Figure 5). These results indicate that adenine methylation induces a distortion or loosening of base pairing in the vicinity of the methylated A. These results also suggest that the destabilization of the

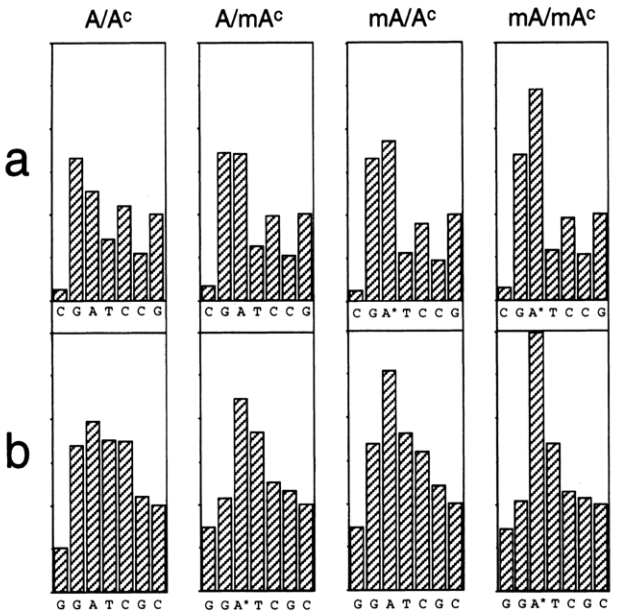

FIGURE 5: Diethyl pyrocarbonate modification of purine bases in the decamer duplex DNA. Densitometric analysis of this modification experiment is shown. This reagent preferentially reacts with N7 of adenines and hence probes the major groove environment of the methylation site. Each panel shows two labeled strands of a decamer duplex, the template strand (a) and the nontemplate strand (b).

decamer duplex DNA by m^6A is due to the local structural alteration in the major groove of the double helix.

The Methylation Site in the Decamer Duplex Binds Ligands Preferentially. We have found that the reagents MPE·Fe^{II} and $(OP)_2Cu^I$ interact preferentially at the branch site in three- or four-arm DNA junctions (reviewed in Lu et al., 1992). It is then of interest to explore the response of the methylation site of the decamer duplexes to cleavage by MPE·Fe^{II} and $(OP)_2Cu^I$. We compare the patterns of scission in a strand of the hemimethylated and fully methylated duplexes with the pattern of a scission of the same strand of the unmethylated duplex. The intercalative probe, MPE·Fe^{II}, a reactive analog of ethidium bromide, binds duplex DNA, cleaving the sugars of the backbone proximal to the binding site (Hertzberg & Dervan, 1984). The results of cleaving the four decamer duplexes are shown in Figure 6A. The fully methylated duplex mA/mA^c and the hemimethylated duplex mA/A^c shows a clear enhancement in MPE·Fe^{II} cleavage at A5, T6, C7, and G8 of the nontemplate strand and A5 in the template strand, relative to the unmethylated control (see Figure 6A). The hemimethylated duplex A/mA^c also shows a minor enhancement at A5 in the nontemplate strand. The enhanced reactivity to MPE·Fe^{II} is consistent with the presence of preferred interaction site for drugs at the methylation site.

$(OP)_2Cu^I$ binds to duplex DNA via the minor groove (Sigman, 1986) and induces radical scission by oxidation of deoxyribose (Kuwabara et al., 1986). Figure 6B shows the cleavage pattern of the unmethylated and methylated decamer duplexes by $(OP)_2Cu^I$. In both of the hemimethylated duplexes, an enhanced cleavage is seen at A5 and T6 in the unmethylated strand as is a protection at T6 in the methylated strand, relative to the unmethylated species (see Figure 6B). The fully methylated duplex shows enhanced scission at position A5 of both strands relative to the unmethylated control (Figure 6B). These cleavage patterns indicate preferential interactions in the vicinity of the methylation site of the decamer duplex.

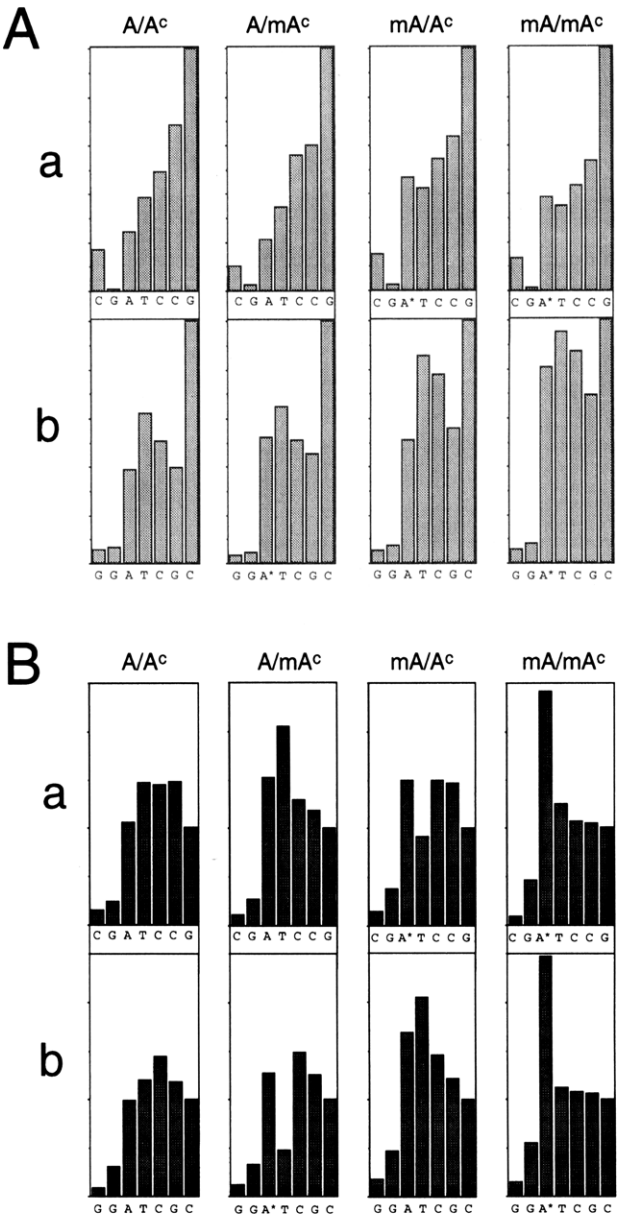

FIGURE 6: Cleavage of the decamer duplexes by MPE·Fe^{II} (A) and $(OP)_2Cu^I$ (B). Densitometric analysis of the cleavage patterns by these chemical reagents is shown. The same conventions apply to this figure as to Figure 5.

DISCUSSIONS

Despite previous spectroscopic and structural investigations, the consequences of methylation of adenine in a DNA duplex remain incompletely understood. In particular, the NMR evidence indicates the presence of some intermediate state in short oligomers, which alters the rate of exchange between duplex and coil. NMR studies require concentrations of strands above 1 mM, and lines tend to broaden at low temperatures. This makes it useful to explore the consequences of adenine methylation in the context of longer oligomers using strands that pair at lower concentrations and temperature, favoring the ordered form(s) of modified duplexes.

Our observations provide evidence that methylation of adenine induces a structural alteration of the duplex in the vicinity of a methylated A in the duplex. First, CD studies show small but discernible differences between the spectra of unmethylated and hemimethylated or fully methylated decamer duplexes (see Figure 3), suggesting structural

perturbations in local conformation and/or dynamics. Second, the DEPC modification experiments suggest that the mA·T base pair is accessible or "open" more frequently than the unmethylated A·T pair in the identical strand background. This result was not seen in an NMR study which shows, at temperatures above 20 °C, that the presence of (hemi)-methylated A increases the lifetime of protons in the duplex, despite destabilizing the overall structure (Fazakerley et al., 1987). Engel and von Hippel (1978) were led to conclude that the destabilizing effect of methylation of A in polydA·dT does not favor looping out or opening at low temperatures. Finally, the MPE·Fe^{II} and $(OP)_2Cu^{I}$ data imply a conformational difference, without specifying the nature of the difference. In addition, the thermodynamic profile for each duplex reveals a reduction in the enthalpy of duplex formation, which is consistent with the notion that pairing and/or stacking in the hemimethylated and fully methylated duplexes is compromised. For example, the compensating entropy could be understood to represent exposure of a base or change in solvation the modified duplex.

While it is premature to attempt to propose a detailed structural model from the evidence at hand, the above features can be reconciled by a simple hypothesis that the methylated adenine base pair in the duplex is in dynamic equilibrium between two paired states of the duplex, in one of which the pairing is Watson−Crick and in the other of which the pairing might be Hoogsteen or some other form. We cannot specify the nature of the pairing in either structure, at this point; the observation in the NMR spectra of methylated and unmethylated duplexes suggests one of these states is close to Watson−Crick. The equilibrium depends on the local sequence; thus the two hemimethylated species need not be equivalent, and the fully methylated duplex can differ from both. The interconversion requires that the methylated A be transiently open, consistent with our observation that residues at the methylation site are hyperreactive to DEPC. The transient opening may also facilitate binding of the methidium ring in MPE, leading to enhanced the rates of scission in the vicinity of the modified site. The fact that the overall helix lifetime increases rather than decreases (Fazakerley et al., 1987) could be ascribed to the fact that the lifetime reflects the contribution from two stable helical states rather than a single one as in A/Ac. In the three-state picture, the time spent unpaired can decrease relative to the simpler two-state system in the unmethylated duplex. For this reason, the overall exchange rate at low temperature can be slow, but would clearly increase with temperature as the strands dissociate. In this picture, the thermodynamic destabilization results from the reduced stability of the Watson−Crick mA·T pair, assuming the alternative pairing (Hoogsteen or other) is about as stable as the Watson−Crick A·T pair in A/Ac. Our hypothesis suggests that the flipping out of cytosine seen in the X-ray structure of Hae III methyltransferase complexed to DNA (Reinsich et al., 1995) may reflect an underlying conformational process in the sequence, rather than occurring only as a consequence of binding to the enzyme. The mechanism of the C transferase requires access of the enzyme to groups normally buried in G·C pairs of DNA (e.g., N3 of C) without forming a destabilized product as in A methylation.

REFERENCES

Cantor, C., Warshaw, M. W., & Shapiro, H. (1970) *Biopolymers 9*, 1059−1077.

Caruthers, M. H. (1982) in *Chemical and Enzymatic Synthesis of Gene Fragments* (Gassen, H. G., & Lang, A., Eds.) pp 71−79, Verlag Chemie, Weinheim, Germany.

Derosiers, R., Friderici, K., & Rottman, F. (1974) *Proc. Natl. Acad. Sci. U.S.A. 71*, 3971−3975.

Engel, J. D., & von Hippel, P. H. (1974) *Biochemistry 13*, 4143−4158.

Engel, J. D., & von Hippel, P. H. (1978) *J. Biol. Chem. 253*, 927−934.

Erie, D. A., Jones, R. A., Olson, W. K., Sinha, N. K., & Breslauer, K. J. (1989) *Biochemistry 28*, 268−273.

Fazakerley, G. V., Teoule, R., Guy, A., & Guschlbauer, W. (1984) *FEBS Lett. 176*, 449−452.

Fazakerley, G. V., Teoule, R., Guy, A., Fritzsche, H., & Guschlbauer, W. (1985) *Biochemistry 24*, 4540−4548.

Fazakerley, G. V., Quignard, E., Teoule, R., Guy, A., & Guschlbauer, W. (1987) *Eur. J. Biochem. 167*, 397−404.

Geier, G. E., & Modrich, P. (1979) *J. Biol. Chem.* 254, 1408−1413.

Gilbert, W., Maxam, A., & Mirzabekov, A. (1976) in *Control of Ribosome Synthesis* (Kjelgaard, N. O., & Maaloe, O., Eds.) pp 139−148, Munksgaard, Copenhagen.

Guo, Q., Seeman, N. C., & Kallenbach, N. R. (1989) *Biochemistry 28*, 2355−2359.

Guo, Q., Lu, M., Seeman, N. C., & Kallenbach, N. R. (1990) *Biochemistry 29*, 570−578.

Herr, W. (1985) *Proc. Natl. Acad. Sci. U.S.A. 82*, 8009−8013.

Hertzberg, R. P., & Dervan, P. B. (1984) *Biochemistry* 23, 3934−3945.

Johnston, B. H., & Rich, A. (1985) *Cell 42*, 713−724.

Kuwabara, M., Yoon, C., Goyne, T., Thederahn, T., & Sigman, D. (1986) *Biochemistry 25*, 7401−7408.

Lu, M., Guo, Q., Seeman, N. C., & Kallenbach, N. R. (1990) *Biochemistry 29*, 3407−3412.

Lu, M., Guo, Q., & Kallenbach, N. R. (1992) *Crit. Rev. Biochem. Mol. Biol. 27*, 157−190.

Lu, M., Campbell, J. L., Boye, E., & Kleckner, N. (1994) *Cell 77*, 413−426.

Lyons, S. M., & Schendel, P. F. (1984) *J. Bacteriol. 159*, 421−423.

Marinus, M. G. (1976) *Mol. Gen. Genet. 128*, 853−854.

Marky, L. A., & Breslauer, K. J. (1987) *Biopolymers 26*, 1601−1620.

Marky, L. A., Kallenbach, N. R., McDonough, K. A., Seeman, N. C., & Breslauer, K. J. (1987) *Biopolymers 26*, 1621−1634.

Modrich, P. (1987) *Annu. Rev. Biochem. 56*, 435−466.

Pukkila, P., Peterson, J., Herman, G., Modrich, P., & Meselson, M. (1983) *Genetics 104*, 571−582.

Quignard, E., Fazakerley, G. V., Teoule, R., Guy, A., & Guschlbaur, W. (1985a) *Eur. J. Biochem. 152*, 99−105.

Quignard, E., Teoule, R., Guy, A., & Fazakerley, G. V. (1985b) *Nucleic Acids Res. 13*, 7829−7836.

Reinisch, K. M., Chen, L., Verdine, G. L., & Lipscomb, W. N. (1995) *Cell 82*, 143−153.

Rinkel, L J., van der Marel, G. A., van Boom, J. H., & Altona, C. (1987a) *Eur. J. Biochem. 163*, 275−286.

Rinkel, L J., van der Marel, G. A., van Boom, J. H., & Altona, C. (1987b) *Eur. J. Biochem. 163*, 287−296.

Roberts, D., Hoopes, B. C., McClure, W. R., & Kleckner, N. (1985) *Cell 43*, 117−130.

Rosenberg, J. M., Seeman, N. C., Kim, J. P., & Rich, A. (1973) *Nature 243*, 150−154.

Russell, D. W., & Zinder, N. D. (1987) *Cell 50*, 1071−1079.

Sigman, D. S. (1986) *Acc. Chem. Res. 19*, 180−186.

Singer, B. (1975) *Prog. Nucleic Acid Res. Mol. Biol. 15*, 219−284.

Slater, S., Wold, S., Lu, M., Boye, E., Skarstad, K., & Kleckner, N. (1995) *Cell* (in press).

Tinoco, I, Jr., & Cantor, C. R. (1970) *Methods Biochem. Anal. 18*, 81−96.

van Dyke, M. W., & Dervan, P. B. (1983) *Nucleic Acids Res. 11*, 5555−5567.

BI9513362